



HAL
open science

Mechanical synthesis of nanostructured $\text{Y}_2\text{Ti}_2\text{O}_7$ pyrochlore oxides

E. Simondon, P-F Giroux, L. Chaffron, A. Fitch, P. Castany, T. Gloriant

► **To cite this version:**

E. Simondon, P-F Giroux, L. Chaffron, A. Fitch, P. Castany, et al.. Mechanical synthesis of nanostructured $\text{Y}_2\text{Ti}_2\text{O}_7$ pyrochlore oxides. *Solid State Sciences*, 2018, 85, pp.54-59. 10.1016/j.solidstatesciences.2018.09.006 . hal-01935361

HAL Id: hal-01935361

<https://univ-rennes.hal.science/hal-01935361v1>

Submitted on 4 Dec 2018

HAL is a multi-disciplinary open access archive for the deposit and dissemination of scientific research documents, whether they are published or not. The documents may come from teaching and research institutions in France or abroad, or from public or private research centers.

L'archive ouverte pluridisciplinaire **HAL**, est destinée au dépôt et à la diffusion de documents scientifiques de niveau recherche, publiés ou non, émanant des établissements d'enseignement et de recherche français ou étrangers, des laboratoires publics ou privés.

AUTHORS

E. Simondon¹, P.-F. Giroux¹, L. Chaffron¹, A. Fitch², P. Castany³, T. Gloriant³

¹ DEN-Service de Recherches Métallurgiques Appliquées, CEA, Université Paris-Saclay, F-91191, Gif-sur-Yvette, France

² ESRF-The European Synchrotron Radiation Facility, CS40220, 38043 Grenoble, France

³ Univ Rennes, INSA Rennes, UMR CNRS 6226 ISCR, 35000 Rennes, France

Corresponding author:

E. Simondon

Tel: +33 01 69 08 80 43

E-mail address: esther.simondon@cea.fr

Postal address: DEN-Service de Recherches Métallurgiques Appliquées, CEA, Université Paris-Saclay, F-91191, Gif-sur-Yvette, France

No color should be used for any figure

Declaration of interest: none

TITLE

Mechanical synthesis of nanostructured $Y_2Ti_2O_7$ pyrochlore oxides

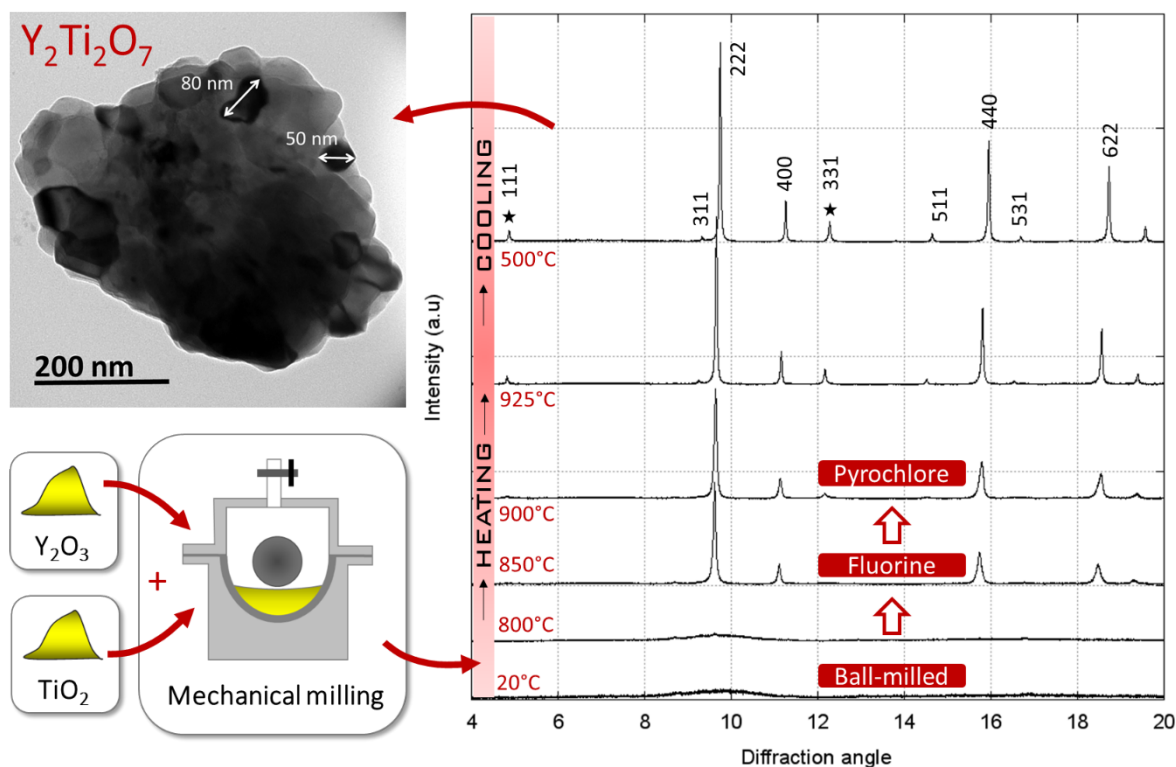
ABSTRACT

Pyrochlore-type $Y_2Ti_2O_7$ powders were synthesized by mechanical milling. Nanosized powders of Y_2O_3 and TiO_2 are milled to form an amorphous mixture of $Y_2Ti_2O_7$ containing a small quantity of crystallized fluorite structure and initial constituents. The desired fully crystallized pyrochlore phase is obtained from this mixture through heat treating at 900°C. In situ X-ray Diffraction by Synchrotron radiation investigations reveal that this transformation takes place through a first step of crystallization into a fluorite-like structure at 800°C. The formation of the pyrochlore structure occurs around 900°C. The obtained product is a nanostructured pyrochlore powder of which can be integrated in the manufacturing process of oxide dispersion strengthened steels.

KEYWORDS

Pyrochlore oxide; Mechanical milling; nanostructure; X-ray diffraction (XRD); Synchrotron radiation

GRAPHICAL ABSTRACT



ARTICLE

1. INTRODUCTION

$\text{Y}_2\text{Ti}_2\text{O}_7$ oxides are part of a large family of $\text{A}_2\text{B}_2\text{O}_7$ oxides displaying pyrochlore structure, where A and B are metal cations. The fully ordered pyrochlore structure presents a cubic symmetry (Space Group: $\text{Fd}\bar{3}\text{m}$) and can be described in terms of a superstructure of the ideal defect fluorite structure (cubic, S.G.: $\text{Fm}\bar{3}\text{m}$) with twice the cell constant ($a \approx 10 \text{ \AA}$) [1].

In this study, $\text{Y}_2\text{Ti}_2\text{O}_7$ pyrochlore oxides are produced and examined to be directly introduced in Oxide-Dispersion-Strengthened (ODS) steel during manufacturing process. The presence of a dense dispersion of this highly stable oxide under irradiation in the ferritic matrix improves mechanical strength and traps irradiation defects [2] [3].

$\text{Y}_2\text{Ti}_2\text{O}_7$ is usually produced by a standard solid state process. This method requires repeated cycles of ball-milling and heat treatments above 1000°C , involving an important growth and aggregation of particles [4] [5]. Among the solid state processes, high-energy ball milling has revealed to be an efficient method to produce complex oxide nanopowders [6] [7] [8]. It has been demonstrated that the process involving repeated ball-powder collision events during the milling could induce mechanochemical solid-state reactions in the milled powder [9] [10]. The repeated welding and fracturing of powder particles increases the area of contact between the reactant powder particles and allows fresh surfaces to come into contact repeatedly. As a consequence, the reaction that normally requires high temperatures to facilitate the diffusion occurs at room temperature during mechanical milling and nanosized particles can be obtained [11].

$Y_2Ti_2O_7$ pyrochlore powders have recently been produced by a simple mechanochemical synthesis technique [12] [13] [14]. Moreno *et al.* [12] showed that a milling of a stoichiometric mixture of Y_2O_3 and TiO_2 powders for 19 h in a zirconia planetary ball mill leads to obtaining a single-phased powder. Fuentes *et al.* [13] and Singh *et al.* [14] showed that the produced as-milled powders were composed by partially disordered phases, which are intermediate between the ordered pyrochlore and disordered fluorite structures. This partially disordered pyrochlore structure transforms into the ordered form around 800°C, mainly due to oxygen re-arrangements [13].

The aim of this contribution is to propose a mechanochemical method to synthesize highly pure $Y_2Ti_2O_7$ powders with an ordered pyrochlore type of structure and nanosized crystallites. After a first step of milling of the initial constituents, a short annealing allows the transformation into the fully ordered pyrochlore phase while limiting the crystallites growth.

2. MATERIALS AND METHODS

Initial powders used in this work were nano-sized TiO_2 (Degussa, 99,5%) and Y_2O_3 (Sigma-Aldrich, 99,9%) powders. They were pelletized into an 8-mm-diameter die under 3 t mass and then submitted to a primary annealing for 10 h under vacuum (10^{-6} mbar at 550°C and 1000°C respectively, in order to remove adsorbed H_2O). Appropriate amount of the as-treated constituent oxides was selected ($Y_2O_3/2TiO_2$) to reach a complete transformation in $Y_2Ti_2O_7$. Batches of 3 g were ball milled in a modified FRITSCH Pulverisette-0 mill with tungsten carbide vial and ball under a static vacuum (10^{-6} mbar) for 120 h with an intensity of 1400 $m.s^{-2}$ [15]. Heat treatments on the as-milled powders were performed under vacuum (10^{-6} mbar) at 900°C with a $10^\circ C.min^{-1}$ temperature ramp followed by an immediate natural cooling. From the first heat treatment of the initial powders to the harvesting of milled and annealed final powders, the samples were at all time handled in a controlled atmosphere (argon or vacuum) in order to prevent any interaction with air. The samples were characterized by X-ray powder diffraction, using a BRUKER D8 diffractometer with Ni-filtered $CuK_{\alpha 1}$ radiation ($\lambda = 1.5406 \text{ \AA}$). The diffraction patterns of the samples were measured over the angular range $13 - 70^\circ$ (2θ) with step size 0.02° and scan speed $0.24^\circ.min^{-1}$. The samples were also examined by thermal analysis in a SETARAM TAG 24 using a typical sample mass of 100 mg and a heating rate of $10^\circ C.min^{-1}$ in argon or air. In situ XRD spectra were collected on beam line ID22 (using $\lambda=0.495992 \text{ \AA}$ wavelength) at the European Synchrotron Radiation Facility (ESRF, Grenoble, France). The scans were performed at $10^\circ.min^{-1}$ from 5 to 20° (2θ) of the central detector, with a 0.5 mm silica-glass capillary, 10 μm wall thickness, spun axially at 787 rpm. The temperature ramp of $10 K.min^{-1}$ was achieved via a hot-air blower. Scanning electron microscopy (SEM) was carried out on a HIROX SH-3500MB microscope working at 20 kV. Transmission electron microscopy (TEM) and selected area electron diffraction (SAED) were performed on a JEOL 2100 working at 200 keV.

3. RESULTS

Fig. 1(a) shows the evolution of the XRD pattern of the $Y_2O_3 + 2TiO_2$ mixture before and after the milling in a high energy ball mill. As a reference, the XRD pattern of the starting mixture (**Fig. 1(a)(i)**) presents peaks from both cubic Y_2O_3 (ICDD card 00-41-1105) and TiO_2 in the form of rutile (01-089-0553) and anatase (00-021-1272). The XRD diffraction pattern of the ball-milled powder (**Fig. 1(a)(ii)**) indicates that the powder is mostly amorphous-like with broad peaks of low intensities and contains a crystalline fraction indicated by a few narrow peaks of low intensity. The decrease in intensity and increase in peak broadening is the result of, on the one hand, a considerable refinement of particle and crystallite size and, on the other hand, the introduction of a large number of structural

defects in the constituent oxides. The diffraction pattern is then decomposed into a baseline (Fig. 1(a)(iii)) representing the amorphous component and the deconvolved signal (Fig. 2(a)(iv)) representing the crystalline fraction. On the baseline pattern (Fig. 1(a)(iii)), the main broad peak roughly correspond to the (222) main reflections of $Y_2Ti_2O_7$ at $2\theta = 30.64^\circ$. On the deconvolved signal (Fig. 1(a)(iv)), the main reflections of anatase TiO_2 and cubic Y_2O_3 are evident, revealing the presence of residual initial constituents.

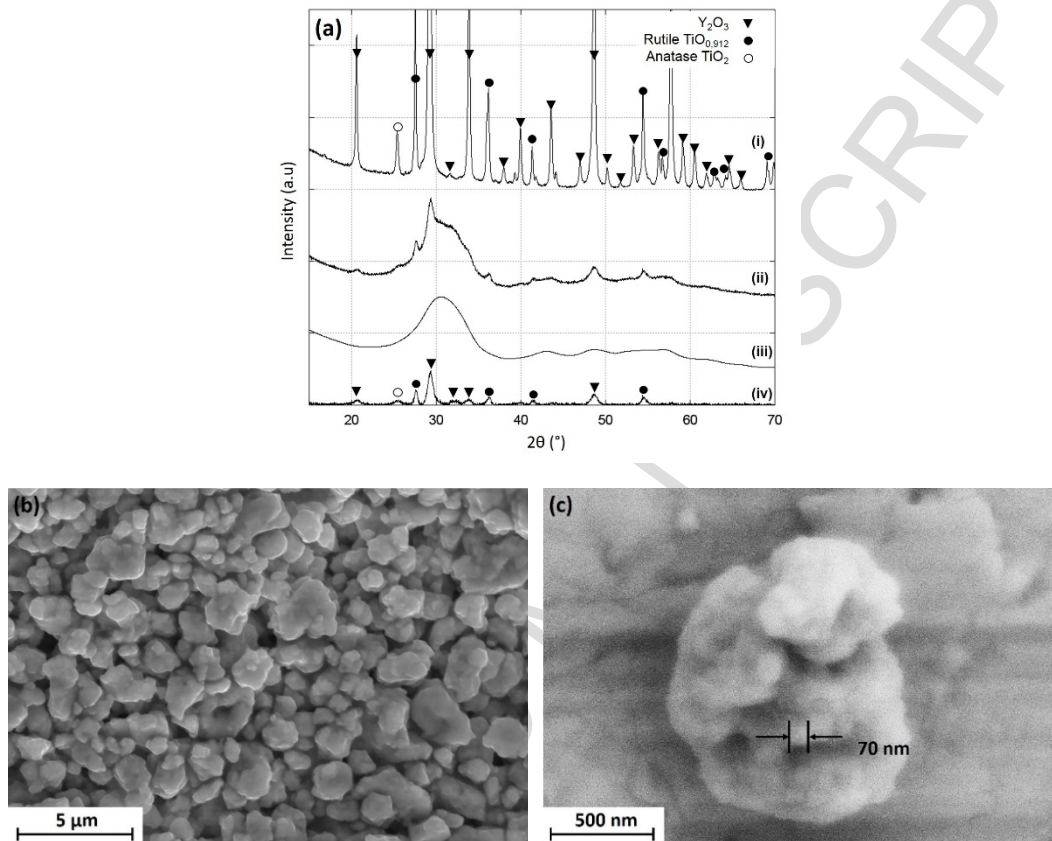


Figure 1 : (a) X-ray diffraction patterns of the starting mixture (i) and the ball-milled powder (ii). The diffractogram (ii) is decomposed in a baseline representing the amorphous component (iii) and the deconvolved signal representing crystalline fractions (iv). (b) and (c) are SEM micrographs of the ball-milled powder at different magnifications.

SEM observations reveal that after the milling, the powder is characterized by a typical morphology of ball-milled ceramic samples composed by sub-micronic agglomerated particles of irregular shape [16] (Fig. 1(b)). They are themselves constituted of nanoparticles agglomerates (Fig. 1(c)). The microstructure of this milled powder was characterized by TEM and SAED. Figs. 2(a) and (b) present observation zones at the edge of two different agglomerates, in bright (Fig. 2(a)) or dark field (Fig. 2(b)) with the associated SAED patterns. In most observed agglomerates, even the diffraction contrast in the micrograph fails to reveal any crystallite within the powder particle, as illustrated in Fig. 2(b). The corresponding SAED diagram presents a very diffuse ring along with some scattered bright spots. The diffuse maxima observed can be explained as a result of small domain size together with poor crystallinity at the atomic scale, or with an amorphous structure. The bright spots correspond to a few crystallites of various natures such as Y_2O_3 or TiO_2 . The powder is then composed mainly of an amorphous phase along with a few un-milled crystallites of remaining initial constituents, which is

consistent with the broad XRD pattern seen above (**Fig. 1(a)**). As illustrated in **Fig. 2(b)**, some crystallites can be visible and the associated SAED patterns are typical of polycrystalline materials (diffraction rings instead of well-defined spots, for all crystallites have random orientations). The interplanar distances correspond to the main reflections (111), (220) and (311) of the fluorite structure. This phenomenon can be explained by the reaction occurring between the constituents during the milling. This mechanically activated reaction is induced by the combined action of shearing and temperature local rise during impacts, which facilitates atomic mobility and initiates transformations that would usually take place during a posterior heat treatment. The milled powder is then not fully crystallized pyrochlore and corresponds to an amorphous phase of $Y_2Ti_2O_7$, along with some small crystallites of fluorite-like structure as well as some remaining crystallites of the initial constituents.

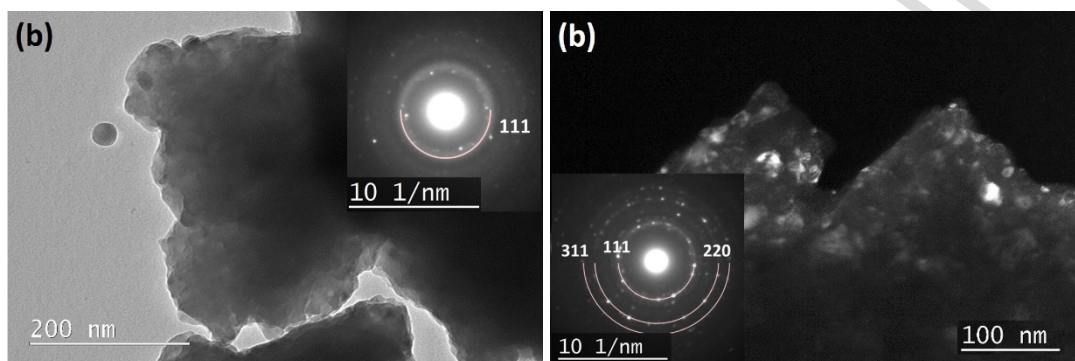


Figure 2 : TEM micrographs of milled powder, associated SAED patterns are shown as insets

Thermodifferential analyses on the milled powders revealed an exothermic event at about 855°C (**Fig. 3(a)**). The main peak is narrow around this temperature and is followed by a much smaller peak on a larger range of temperature (880°C - 1000°C). As a comparison, the un-milled initial mixture does not show any peak in DTA spectra. Moreover, the exothermic transformation is found to be non-reversible. To highlight the origin of the exothermic event identified by DTA, the milled powder was characterized by XRD under Synchrotron radiation at ESRF Grenoble. **Fig. 3(b)** presents XRD patterns of the milled powder at several temperatures during the heat treatment from bottom to top: heating from 20°C to 925°C and then cooling to 500°C . **Fig. 3(c)** looks more closely on the patterns run between 790°C and 830°C while heating. The XRD pattern of the sample remains nearly identical to the initial milled powder from room temperature to about 800°C . Starting from 800°C , characteristic diffracted peaks of a fluorite-like phase start to appear, and their number and intensity increase with rising temperature (**Fig. 3(c)**). The pyrochlore structure can be considered as a superstructure of an anion deficient fluorite-like atomic arrangement with twice the cell constant. Therefore, its diffraction pattern is composed by (i) a set of strong intensities characteristic of the underlying fluorite-type average structure and (ii) an additional set of superstructure reflections with intensities depending on several factors (degree of ordering, difference in average scattering factors of the elements involved, distribution of oxygen vacancies, etc...). For $Y_2Ti_2O_7$, according to the comparison between ICDD card 04-015-3376 for pyrochlore and 04-008-1806 for fluorite, the main superstructure visible peaks correspond to (111) and (331). There are labeled with a star on **Fig. 3(b)** and are only visible above the 900°C temperature patterns.

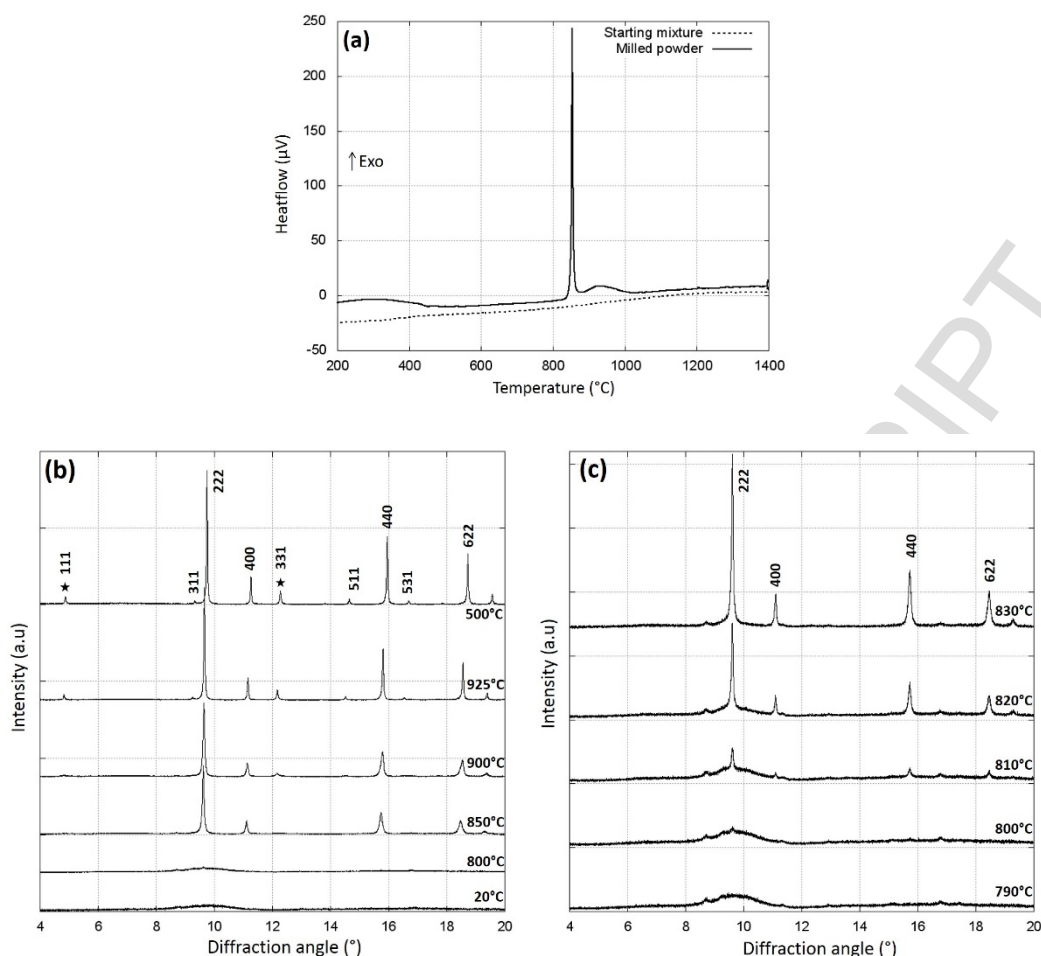


Figure 3 : (a) Differential thermal analysis (10°C/min) of the initial mixture and of the as-milled powder. In situ XRD of the as-milled powder (b) heating from 20°C to 925°C and cooling to 500°C from bottom to top, (c) zoom on heating from 790°C to 830°C. Labelled peaks are pyrochlore-like structure, and the superstructure peaks are labelled with a star.

As previous observations demonstrate that fully ordered pyrochlore structure $Y_2Ti_2O_7$ is synthesized with an annealing treatment at more than 850°C, the powder was heat treated at 900°C in a pyrolysis oven under vacuum with a 10°C.min⁻¹ heating ramp and immediate natural cooling to prevent crystallite growth. The XRD pattern of the obtained powder is presented in **Fig. 4(a)**. As a reference, the as-milled powder XRD pattern before annealing is also presented. After the annealing, the XRD pattern matches the one expected for pyrochlore-type $Y_2Ti_2O_7$ (ICDD card 04-015-3376) and no extra peaks are observed. In particular, Y_2O_3 and TiO_2 peaks are not visible anymore, which is proof of a total transformation. The superstructure peaks of pyrochlore at $2\theta=15.18^\circ$ and $2\theta=38.84^\circ$ are clearly visible. These observations confirm the results obtained with Synchrotron experiments. TEM observations have been performed on several observation zones on the heat treated powder, showing nanocrystallites on the range of 50 to 80 nm (**Fig. 4(b)**). SAED patterns enable to identify the pyrochlore $Y_2Ti_2O_7$ structure (**Fig. 4(c)**), confirming the XRD results. From XRD pattern shown in **Fig. 4(a)**, the average crystallite size of sample calculated using Scherrer's equation is 50.6 nm [17], which is consistent with the TEM observations in **Fig. 4(b)**.

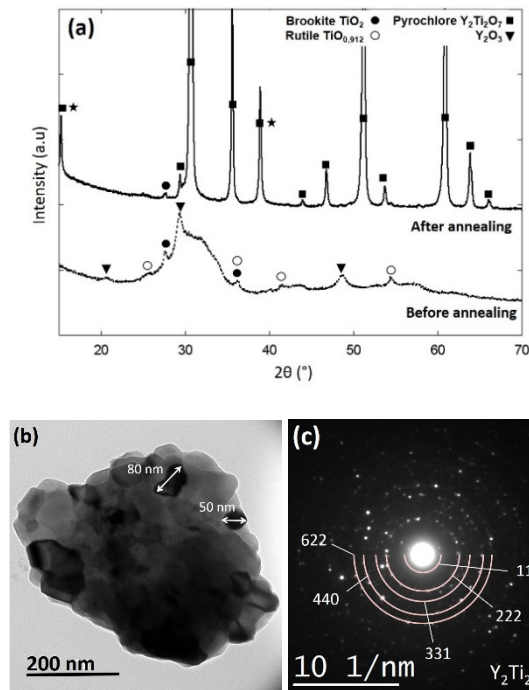


Figure 4 : (a) X-ray diffraction patterns of ball-milled powder before and after annealing at 900°C . (b) TEM micrograph of powder after annealing at 900°C and (c) SAED pattern of the same sample

4. DISCUSSION

Milling a stoichiometric mixture of Y_2O_3 and TiO_2 produces a mostly amorphous-like mixture of $Y_2Ti_2O_7$ containing small crystallites of both initial constituents and fluorite-like structures. Previous studies have showed that, after 9h of milling with different conditions (type of miller, milling media, atmosphere...), the XRD pattern of the milled powder is composed only by the peaks of a pyrochlore-like structure [13] [12] [14]. The mechanically activated chemical reaction between Y_2O_3 and TiO_2 proceeds through an initial step of particle and crystallite size reduction of the starting oxides, together with the polymorphic transformation from cubic to monoclinic Y_2O_3 . The formation of the pyrochlore $Y_2Ti_2O_7$ seems to take place as a second step from an amorphous matrix of these oxides [13].

The selected milling conditions of the present study do not enable to the occurrence of the crystallization of the milled powder from an amorphous form to a pyrochlore-like structure directly in the mill, even after a long time run (240 h). This phenomenon could be explained by the use of tungsten carbide as a milling media instead of zirconia. Several studies have showed that compared to other milling medias (stainless steel and tungsten carbide), zirconia induces faster reactions [18] [19] [20]. Because of its rather low thermal conductivity, the heat produced during milling using the zirconia milling media is assumed to be effectively stored, and the ignition temperature can be reached within a shorter time. However, zirconia is less resistant than tungsten carbide and can introduce a pollution from 2 to 4% in the powder [13]. The increase in Zr content in the powder increases disorder [12], which is not in line with the synthesis of a stable and pure powder of $Y_2Ti_2O_7$ oxide with a pyrochlore structure of this study.

In this study, the heat treatment of the milled powder enables to synthesize the fully crystallized pyrochlore phase from a mostly amorphous structure. According to DTA, crystallization occurs around $855^\circ C$ as revealed by a sharp exothermic event. However, previous calorimetry studies of ball-milled $Y_2Ti_2O_7$ attribute this exothermic event to atomic ordering [13] [14]. During heating, the partially disordered pyrochlore phase (which is an intermediate between the ordered pyrochlore and disordered fluorite) forms the pyrochlore lattice. In the present study, the ball-milled sample is composed by an amorphous powder. As a consequence, the sharp exothermic peak could be associated to crystallization of the Y-Ti-O oxides and the second broader peak to rearrangement and redistribution of cations and oxygen ions. Measurements performed in Synchrotron show a crystallization of a fluorite-like structure around $800^\circ C$, and then formation of the pyrochlore superstructure around $900^\circ C$. This is consistent with the previous observation and interpretation of DTA. The difference between the crystallization temperatures measured by Synchrotron and DTA analysis can be explained by slight differences in experimental conditions (atmosphere, thermocouple position, measurements sensitivity...).

CONCLUSION

In order to form a nanosized powder of $Y_2Ti_2O_7$ oxide with pyrochlore structure, ceramic powders of Y_2O_3 and TiO_2 were milled in a high energy ball mill for 120 h. The obtained ball-milled powder is composed by sub-micronic agglomerated particles of irregular shape, themselves constituted of nanoparticle agglomerates. The XRD analysis reveals the obtained milled-powder to be a stoichiometric amorphous mixture of $Y_2Ti_2O_7$ containing a small quantity of crystallized fluorite structure and initial constituents. The Synchrotron and DTA study enabled to observe the crystallization of the amorphous mixture into a fluorite-like phase around $800^\circ C$ followed by a rearrangement forming the pyrochlore structure around $900^\circ C$ with rising temperature. After the cooling, the sample is pure and composed of nanostructured pyrochlore powder.

ACKNOWLEDGEMENT

This work was supported by CEA in the framework of the MACNA project. The authors would like to thank Patrick Bonnaillie for the SEM characterizations.

REFERENCES

- [1] M. A. Subramanian, G. Aravamudan, and G. V. Subba Rao, "Oxide pyrochlores - A review," *Progress in Solid State Chemistry*, vol. 15, no. 2, pp. 55–143, 1983. [https://doi.org/10.1016/0079-6786\(83\)90001-8](https://doi.org/10.1016/0079-6786(83)90001-8)
- [2] R. L. Klueh, J. P. Shingledecker, R. W. Swindeman, and D. T. Hoelzer, "Oxide dispersion-strengthened steels: A comparison of some commercial and experimental alloys," *Journal of Nuclear Materials*, vol. 341, no. 2–3, pp. 103–114, 2005. <https://doi.org/10.1016/j.jnucmat.2005.01.017>
- [3] T. Yamamoto et al., "The transport and fate of helium in nanostructured ferritic alloys at fusion relevant He/dpa ratios and dpa rates," *Journal of Nuclear Materials*, vol. 367–370, pp. 399–410, 2007. <https://doi.org/10.1016/j.jnucmat.2007.03.047>
- [4] S. X. Wang, L. M. Wang, R. C. Ewing, and K. V. Govindan Kutty, "Ion irradiation of rare-earth- and yttrium-titanate-pyrochlores," *Nuclear Instruments and Methods in Physics Research Section B: Beam Interactions with Materials and Atoms*, vol. 169, no. 1, pp. 135–140, 2000. [https://doi.org/10.1016/S0168-583X\(00\)00030-6](https://doi.org/10.1016/S0168-583X(00)00030-6)
- [5] M. A. Hayward, "Phase Separation during the Topotactic Reduction of the Pyrochlore $Y_2Ti_2O_7$," *Chem. Mater.*, vol. 17, no. 3, pp. 670–675, 2005. <https://doi.org/10.1021/cm048220p>
- [6] V. Zyryanov, "Mechanochemical synthesis of complex oxides," *Russian Chemical Reviews*, vol. 77, no. 2, pp. 105–135, 2008.
- [7] A. C. Dodd and P. G. McCormick, "Synthesis of nanocrystalline ZrO_2 powders by mechanochemical reaction of ZrC_{14} with $LiOH$," *Journal of the European Ceramic Society*, vol. 22, no. 11, pp. 1823–1829, 2002. [https://doi.org/10.1016/S0955-2219\(01\)00500-3](https://doi.org/10.1016/S0955-2219(01)00500-3)
- [8] Z.-F. Fu, P. Liu, X.-M. Chen, J.-L. Ma, and H.-W. Zhang, "Low-temperature synthesis of $Mg_4Nb_2O_9$ nanopowders by high-energy ball-milling method," *Journal of Alloys and Compounds*, vol. 493, no. 1, pp. 441–444, 2010. <https://doi.org/10.1016/j.jallcom.2009.12.122>
- [9] N. J. Calos, J. S. Forrester, and G. B. Schaffer, "A Crystallographic Contribution to the Mechanism of a Mechanically Induced Solid State Reaction," *Journal of Solid State Chemistry*, vol. 122, no. 2, pp. 273–280, 1996. <https://doi.org/10.1006/jssc.1996.0113>
- [10] L. Takacs, "Solid state reactions induced by ball milling," *Hyperfine Interactions*, vol. 111, no. 1, pp. 245–250, 1998. <https://doi.org/10.1023/A:1012670104517>
- [11] C. Suryanarayana, "Mechanical alloying and milling," *Progress in Materials Science*, vol. 46, no. 1, pp. 1–184, 2001. [https://doi.org/10.1016/S0079-6425\(99\)00010-9](https://doi.org/10.1016/S0079-6425(99)00010-9)
- [12] K. J. Moreno, R. S. Rodrigo, and A. F. Fuentes, "Direct synthesis of $A_2(Ti_{1-y}Zr_y)_2O_7$ ($A = Gd^{3+}, Y^{3+}$) solid solutions by ball milling constituent oxides," *Journal of Alloys and Compounds*, vol. 390, no. 1–2, pp. 230–235, 2005. <http://dx.doi.org/10.1016/j.jallcom.2004.07.059>

- [13] A. F. Fuentes, K. Boulahya, M. Maczka, J. Hanuza, and U. Amador, "Synthesis of disordered pyrochlores, $A_2Ti_2O_7$ ($A=Y, Gd$ and Dy), by mechanical milling of constituent oxides," *Solid State Sciences*, vol. 7, no. 4, pp. 343–353, 2005. <https://doi.org/10.1016/j.solidstatesciences.2005.01.002>
- [14] M. Singh, J. K. Gill, S. Kumar, and K. Singh, "Preparation of $Y_2Ti_2O_7$ pyrochlore using high-energy ball milling and their structural, thermal and conducting properties," *Ionics*, vol. 18, no. 5, pp. 479–486, 2012. <https://doi.org/10.1007/s11581-011-0638-z>
- [15] Y. Chen, M. Bibole, R. Le Hazif, and G. Martin, "Ball-milling-induced amorphization in $NiXZrY$ compounds: A parametric study," *Physical Review B*, vol. 48, no. 1, pp. 14–21, 1993.
- [16] S. Bégin-Colin, T. Girot, G. L. Caër, and A. Mocellin, "Kinetics and Mechanisms of Phase Transformations Induced by Ball-Milling in Anatase TiO_2 ," *Journal of Solid State Chemistry*, vol. 149, no. 1, pp. 41–48, 2000. <http://dx.doi.org/10.1006/jssc.1999.8491>
- [17] A. L. Patterson, "The Scherrer Formula for X-Ray Particle Size Determination," *Physical Review*, vol. 56, no. 10, pp. 978–982, 1939.
- [18] B. K. Yen, T. Aizawa, and J. Kihara, "Influence of Powder Composition and Milling Media on the Formation of Molybdenum Disilicide by a Mechanically Induced Self-Propagating Reaction," *Journal of the American Ceramic Society*, vol. 79, no. 8, pp. 2221–2223, 1996. <https://doi.org/10.1111/j.1151-2916.1996.tb08966.x>
- [19] K. Kudaka, K. Iizumi, T. Sasaki, and H. Izumi, "Effect of Milling Media on the Reaction Kinetics of the Mechanochemical Synthesis of Pentatitanium Trisilicide," *Journal of the American Ceramic Society*, vol. 83, no. 11, pp. 2887–2889, 2000. <https://doi.org/10.1111/j.1151-2916.2000.tb01655.x>
- [20] S. Bégin-Colin, G. Le Caër, M. Zandona, E. Bouzy, and B. Malaman, "Influence of the nature of milling media on phase transformations induced by grinding in some oxides," *Journal of Alloys and Compounds*, vol. 227, no. 2, pp. 157–166, 1995. [https://doi.org/10.1016/0925-8388\(95\)01596-5](https://doi.org/10.1016/0925-8388(95)01596-5)